Posture-induced changes in peripheral nerve stiffness measured by ultrasound shear-wave elastography

Article (Accepted Version)

Posture-induced changes in peripheral nerve stiffness measured by ultrasound shear-wave elastography

Authors:

Jane Greening PhD MCSP, Andrew Dilley PhD

Affiliation:

Division of Clinical and Laboratory Investigation, Brighton and Sussex Medical School, Medical Research Building, University of Sussex, Falmer, Brighton BN1 9PS, United Kingdom

Corresponding author:

Andrew Dilley

Division of Clinical and Laboratory Investigation,

Brighton and Sussex Medical School,

Medical Research Building, University of Sussex,

Falmer,

Brighton BN1 9PS,

United Kingdom

Tel: +44 (0)1273 877094

Fax: +44 (0)1273 877884

Email: a.dilley@bsms.ac.uk

Running title: Nerve shear-wave elastography

Keywords: shear-wave elastography, median nerve, tibial nerve, nerve stretch, posture, ultrasound

This article has been accepted for publication and undergone full peer review but has not been through the copyediting, typesetting, pagination and proofreading process which may lead to differences between this version and the Version of Record. Please cite this article as an 'Accepted Article', doi: 10.1002/mus.25245

ABSTRACT

Introduction: Peripheral nerves slide and stretch during limb movements. Changes in nerve stiffness associated with such movements have not been examined in detail but may be important in understanding movement-evoked pain in patients with a variety of different musculoskeletal conditions. Methods: Shear-wave elastography was used to examine stiffness in the median and tibial nerves of healthy individuals during postures used clinically to stretch these nerves. Results: Shear-wave velocity increased when limbs were moved into postures that are thought to increase nerve stiffness (mean increase: median nerve = 208% in arm, 236% in forearm; Tibial nerve = 136%). There was a trend toward a negative correlation between age and shear-wave velocity (r = 0.58 for tibial nerve). Discussion: Shear-wave elastography provides a tool for examining nerve biomechanics in healthy individuals and patients. However, limb position, age, and effects of nerve tension on neural architecture should be taken into consideration.

INTRODUCTION

Peripheral nerves are viscoelastic structures that have to adapt, by sliding and stretching, to changes in limb position. There has been considerable interest in how nerves adapt to limb posture, largely because limb movements that stretch peripheral nerves may result in pain in a variety of clinical conditions including carpal tunnel syndrome, chronic whiplash, and non-specific arm and back pain and diabetic neuropathy.[1, 2, 3, 4] Examples of tests that stretch peripheral nerves include the upper limb tension test 1, which applies stretch to the brachial plexus and the median nerve, and the straight leg raise, which stretches the sciatic nerve. The mechanisms that lead to painful symptoms in response to nerve stretch are not fully understood. It has been suggested that nerve entrapment leads to local increases in nerve stretch during limb movements, which may affect neural function.[5, 6, 7] However, ultrasound studies that have looked for an entrapment of the median nerve at the wrist in patients with carpal tunnel syndrome have been inconclusive. Changes in longitudinal median nerve movement in response to finger and wrist extension have been reported in some studies[8, 9] but not in others.[10] Similarly, we have been unable to identify significant changes in longitudinal median nerve sliding in patients with non-specific arm pain compared to controls.[11] A possible explanation for these discrepancies may be that nerve movements themselves are generally small, and in patients, nerves may be restricted from sliding but the nerve itself may not be “entrapped”.

As a peripheral nerve is stretched, stiffness in that nerve will also increase. Changes in nerve stiffness during limb movements that apply stretch to nerve trunks have not been examined in any detail. Measurements of nerve stiffness may provide additional information on how nerves adapt to joint rotations, as well as the possible biomechanical changes (e.g. changes in *in situ* nerve tension as well as nerve tension during limb movements) that may occur in patients with peripheral neuropathy, such as those with suspected nerve entrapment or diabetic neuropathy. Tissue stiffness can be measured non-invasively using ultrasound elastography. There have been a number of significant developments in ultrasound elastography, including implementation of acoustic radiation force impulse elastography (or shear-wave elastography) in several commercial scanners. Acoustic radiation force impulse technology utilizes high intensity acoustic pulses to mechanically excite tissues, which leads to the generation of shear-waves perpendicular to the acoustic pulse. This technology has been used to delineate nerve trunks from surrounding tissue.[12] Measurement of shear-wave velocity may be

proportional to tissue stiffness.[13] Although shear-wave elastography has been employed to examine musculoskeletal structures such as tendons[14-18] and muscle,[19, 20] there are very few studies on peripheral nerves. The majority of previous studies have instead employed static (compression) elastography, which has been used to examine median nerve stiffness in carpal tunnel syndrome[21-23] and tibial nerve stiffness in diabetic neuropathy.[24] This technique is subject to operator dependence, since it requires the investigator to manually compress the tissue. To date, only 2 studies have used shear-wave elastography to examine the peripheral nervous system. They have focused on the median nerve at the carpal tunnel in patients with carpal tunnel syndrome,[25] and the tibial nerve in ankle dorsiflexion.[26]

In this study, we used shear-wave elastography to explore the feasibility of measuring median and tibial nerve stiffness during limb movements in order to gain a better understanding of the mechanical properties of peripheral nerves. We focused specifically on 2 nerve movement tests that are used clinically, namely the upper limb tension test [1] and the straight leg raise.

METHODS

Subject details. Healthy subjects were recruited for the study. All were examined clinically and questioned to exclude systemic illness, musculoskeletal disorders (e.g. tendinopathy, joint, or muscle injuries), or nerve entrapment syndromes. Twenty-six subjects were included in the main data set (table 1). This study was approved by the local ethical committee, and informed consent was obtained from all subjects.

Ultrasound imaging. During imaging, room temperature was maintained at 21°C. Elastography was carried out using a Siemens Acuson S2000 ultrasound system (Siemens Healthcare, Erlangen, Germany) with a 4-9 MHz 38.5 mm linear array (3 x 192 elements) transducer, which uses acoustic radiation force impulse elastography (Virtual Touch^{TM}) to determine tissue stiffness. Briefly, the ultrasound transducer emits 2 4-MHz, 17 µs acoustic push pulses at 1 edge of a region of interest (ROI). The push pulses mechanically excite the tissue, which leads to generation of shear-waves that propagate through the tissue perpendicular to the acoustic pulse. Tissue displacement triggered by

the shear-waves is measured by 4 paired 6.15 MHz B-mode tracking beams that are emitted at 1mm intervals, 2 mm from the push pulse. An autocorrelation algorithm compares the echoes generated by the tracking beams, and the resulting displacement data areused to determine the speed of the shear-waves passing through the region of excitation (up to 10 m/s), which is proportional to tissue stiffness. This cycle is repeated at 64 equally-spaced lateral intervals (0.6mm) across the ROI. The resulting data are used to construct a 2-dimensional elastogram.[13]

In each subject, the median nerve was imaged anteriorly over the mid-forearm and immediately proximal to the elbow in the upper arm on the dominant side. In the same subjects, the tibial nerve was imaged immediately proximal to the tarsal tunnel on the same side. The ultrasound transducer was positioned longitudinally over the nerve with the marker pointing cephalic. We found during preliminary studies that it was not possible to obtain reliable data in transverse orientation. All the imaging sites chosen represent areas where it was relatively easy to distinguish the peripheral nerve trunk from surrounding soft tissue and, importantly, where nerve trunk movement remained longitudinal in response to limb movements that resulted in increased nerve tension. For each imaging session, the depth setting on the ultrasound was set to 4 cm. All median nerve imaging was performed by the same investigator (JG), and all tibial nerve imaging was performed by AD. B-mode images were also obtained.

Limb positioning. Each subject was imaged in the supine position. For imaging of the median nerve, the upper limb was initially positioned (position 1) with the shoulder abducted to 30°, elbow flexed to 90°, and the wrist in maximum flexion (50-60°). This position was chosen, because it shortens the median nerve path length, i.e. slackens the nerve. The limb was then repositioned into 3 additional postures that incrementally increase the nerve path length. In position 2, the shoulder was abducted to 90°, while maintaining 90° elbow flexion and maximum wrist flexion. This position was only performed in 18 subjects as a single repeat and was therefore not included in the main data analysis. In position 3, the wrist was extended to end of range (60-70°), while maintaining 90° shoulder abduction and 90° elbow flexion. In position 4, the elbow was extended maximally (135-190°), while maintaining 90° shoulder abduction and maximum wrist extension (i.e. end posture for the upper limb tension test 1; figure 1). For tibial nerve imaging, the lower limb was initially positioned (position 1)

with the hip neutral, knee flexed to 90°, and foot neutral. This position was adopted by lowering the leg off the end of the examination couch. It was chosen, because it shortens the tibial nerve bed length, i.e. slackens the nerve. The limb was then repositioned into 2 additional postures that incrementally increased the nerve path length. In position 2, the knee was maximally extended, and the ankle was dorsiflexed to end of range, while maintaining the hip in neutral. In position 3, the hip was positioned into maximum flexion (40-90°), while maintaining maximum knee extension and ankle dorsiflexion (i.e. end position of the straight leg raise; figure 1). Joints were passively held in place using foam supports and by the experimenter. The end range of elbow extension and hip flexion was the maximum angle tolerated by each subject. Each sequence of limb positions was repeated 3 times to obtain repeat measures. Initially, the median nerve was imaged in the forearm, followed by the upper arm, which was followed by imaging of the tibial nerve. For each subject, the sequence of limb positions was the same, except in 18 subjects, when position 2 was added to the upper limb sequence.

Pressure testing. The effects of probe pressure were examined in 3 subjects over the median nerve in the mid-forearm. Each subject was positioned supine with the shoulder abducted to 90°, elbow extended, and wrist neutral. Initially, “light” probe pressure was applied by holding the probe above the skin in excess ultrasound gel. This was followed by “firm” probe pressure, where the investigator applied substantial pressure onto the surface of the skin. Lastly, “moderate” pressure was applied, whereby the probe was resting on the surface of the skin. The sequence was repeated 3 times. As an indicator of probe pressure, the distance from the surface of the transducer to the top of the nerve was measured.

Analysis and statistics. Data were analyzed using SPSS software (IBM, New York, NY, USA). All data were tested for normality. The average nerve shear-wave velocity (m/s) was determined for each image, which was calculated from individual values obtained at 4 equidistant ROIs (size = 1.5 mm x 1.5 mm) along the imaged nerve. Two-way mixed, intraclass correlation coefficients (ICC), with 95% confidence intervals, as well as the within-subject standard deviations (s_w) were calculated from these values as an indication of test-retest reliability. The average of the 3 repeat trials, unless stated, was

used for further statistical analysis. Data were also normalized as a percent change in nerve shear-wave velocity from position 1, i.e. the slack position. Nerve shear-wave velocities in different limb positions were compared using repeated measures analysis of variance (ANOVA) followed by Bonferroni *post hoc* tests. The angle of the nerve across the screen in different limb positions and between trials was also compared using repeated measures ANOVA. Median nerve shear-wave velocities in the upper arm and forearm and repeat testing on different days were compared using paired *t*-tests. Unpaired *t*-tests were used to compare shear-wave velocity with imaging time of day and with gender. The relationship between elbow angle, hip angle, and angle of nerve across the image with the individual shear-wave velocity data for each trial were determined using Spearman rank (r_s) correlation coefficients followed by ANOVA. The association between age and height with mean shear-wave velocity data was assessed using Pearson (r) correlation coefficients, followed by ANOVA. Data are expressed as mean ± SEM unless otherwise stated.

RESULTS

Demographic data. The demographic data are presented in table 1. There was no difference in age between men and women participants, although both weight and height were significantly greater in men. The mean body mass index (BMI) was 23.7 ± 3.7 (SD) (range = 18.0 – 33.6). Two subjects had a BMI above 30. None of the subjects had undertaken vigorous exercise prior to imaging.

Effects of upper limb position on median nerve shear-wave velocities. The data are summarized in figure 2. In position 1, the mean median nerve shear-wave velocity was 2.22 ± 0.07 m/s in the upper arm and 2.61 ± 0.08 m/s in the forearm, a difference that was significant. Position 2 caused negligible change in the median nerve shear-wave velocity in the upper arm (mean = 2.59 ± 0.11 m/s), whereas in the forearm, there was a small but significant decrease. In position 3, there was an increase in median nerve shear-wave velocity in the upper arm (mean = 3.10± m/s) and forearm (mean = 5.87 ± 0.19 m/s). In this position, the percent increase from position 1 was significantly higher in the forearm (127 ± 7%) compared to the upper arm (40 ± 4%). Position 4 caused a substantial increase in median nerve shear-wave velocity in both the upper arm (mean = 6.80 ± 0.31

m/s; percent increase from position 1 = 208 ± 13%) and forearm (mean = 8.65 ± 0.19 m/s; percent increase from position 1 = 236 ± 10%). The mean elbow angle in this position was 179 ± 9.7° (SD). Elbow angle did not correlate with median nerve shear-wave velocity in the forearm (r_s = 0.16, *P* = 0.17) or upper arm (r_s = 0.19, *P* = 0.10). Example elastograms for the start and end limb position are shown in figure 1.

Effects of lower limb position on tibial nerve shear-wave velocities. These are summarized in figure 3. In position 1, the mean tibial nerve shear-wave velocity proximal to the tarsal tunnel was 3.25 ± 0.10 m/s. Position 2 caused a 60 ± 6% increase in tibial nerve shear-wave velocity (mean = 5.16 ± 0.21 m/s), an increase that was significant. In position 3, there was a further increase (136 ± 9% from position 1) in tibial nerve shear-wave velocity (mean = 7.57 ± 0.28 m/s). The mean angle of hip flexion in this position was 62 ± 15.6° (SD). Hip angle did not correlate with tibial nerve shear-wave velocity (r_s = 0.22). Example elastograms for each limb position are shown in figure 1.

Test-retest reliability. Intraclass correlation coefficients (ICC) and within-standard deviations (s_w) for the repeat trials (n = 3) are summarized in tables 2 and 3. In 4 subjects, imaging was repeated 1-12 days after the initial session (table 4). For these subjects, no differences were observed in shear-wave velocities for the median or tibial nerves between the repeat sessions (*P*>0.08, paired *t*-tests).

Analysis of the individual shear-wave velocity measurements obtained from each image showed no observable difference between the proximal 2 velocities (left hand side of image) compared to the distal 2 velocities (right hand side of image; *P*>0.08; paired *t*-tests).

Effects of probe pressure and nerve angle on shear-wave velocity measurements. Shear-wave velocities for the median nerve in the forearm were obtained in 3 subjects with varying degrees of probe pressure (see figure 4). There was <16% change in shear velocity comparing firm to light probe pressure [mean = 5 ± 11% (SD)].

There was no significant correlation between angle of the nerve across the image and shear-wave velocity for the median nerve in the forearm (position 1: r_s = -0.22, *P* = 0.06; position 3: r_s = -0.13, *P* = 0.27; position 4: r_s = -0.07, *P* = 0.55) or the tibial nerve (position 1: r_s = 0.10, *P* = 0.42; position 2: r_s = -0.21, *P* = 0.09; position 3: r_s = -0.22, *P* = 0.08). There was also no observable difference in nerve angle between each trial for both nerves. For the median nerve, there was no significant difference in nerve angle between limb positions. However, the nerve angle was significantly different between positions for the tibial nerve (*P* = 0.02).

Effects of gender, age and height on nerve shear-wave velocities. Gender data are summarized in table 5. For the median nerve, there was no significant difference in shear-wave velocity between men and women in any position in the upper arm or forearm. However, for the tibial nerve, there was a significant increase in shear-wave velocities in men compared to women in position 1.

There were moderate negative correlations between age and shear-wave velocities (i.e. shear-wave velocity decreases with increasing age) for the median nerve in positions 3 (r = 0.57) and 4 (r = 0.45) and the tibial nerve in position 2 (r = 0.58), which were all significant (*P* <0.05, figure 5). For the tibial nerve, there was also a moderate positive correlation between shear-wave velocity and participant height in position 2 only (r = 0.59, *P*<0.05; figure 6). There were no other significant correlations.

DISCUSSION

These results show that increased nerve stretch significantly alters shear-wave velocity, which is consistent with an increase in stiffness. These findings may have implications for the use of elastography for examination of conditions that affect the peripheral nervous system.

Effects of limb position on shear-wave velocity. A major finding was that shear-wave velocities for both the median and tibial nerves increased in postures that lengthen the nerve path. This result is consistent with an increase in nerve stretch, which would lead to an increase in stiffness in such postures.[27] The sequence of limb positions that were performed incrementally extended the nerve

bed, which enabled the effect of individual joint rotations on shear-wave velocity to be determined. For the median nerve, abducting the shoulder with the elbow and wrist flexed caused negligible change in shear-wave velocity in the upper arm or forearm, indicating no change in nerve tension (i.e. the nerve remained slack). This may well be due to the anatomy of the brachial plexus, the configuration of which can accommodate the increase in nerve path length during shoulder abduction. With the addition of wrist extension, there was a significant increase in shear-wave velocity in the upper arm and forearm, consistent with a further increase in nerve path length and subsequent stretching of the nerve. The substantial difference in shear-wave velocity between the forearm and upper arm in this position may represent increased stretching of the median nerve closer to the moving joint. Across individual images, significant differences in shear-wave velocity could not be detected. The final upper limb position (position 4), which also corresponds to the final position of the upper limb tension test 1, produced an additional increase in nerve shear-wave velocity that was consistent with further stretching of the median nerve. Overall, there was >200% increase in median nerve shear-wave velocity in the upper arm and forearm with the limb in an extended posture (position 4) compared to the non-tensioned position (position 1). This estimate is likely to be an underestimation, because in some subjects there was a degree of saturation where the shear-wave velocity exceeded 10 m/s (see methods). In a previous study we showed a 3-4% increase in nerve strain in this extended limb position.[27] Taken together, small changes in nerve strain, and therefore stiffness, can cause large increases in shear-wave velocity. While it would be expected that the fully extended position of the upper limb would cause an increase in nerve stiffness, it is surprising that even with the elbow flexed, wrist extension alone is sufficient to increase nerve shear-wave velocity proximal to the elbow. The ease with which nerve stiffness is altered by limb position may have a significant impact on endoneurial blood flow, and possibly neural function, if such limb postures are maintained for prolonged periods. Consistent with the pattern of shear-wave velocity for the median nerve, the tibial nerve showed similar increases in shear-wave velocity from the slack (position 1) to the tensioned nerve position (position 3), with an increase of 136% in position 3. This final position of hip flexion and ankle dorsiflexion represents the end point of the straight leg raise, a clinical test that is used to determine the mechanical sensitivity of the sciatic nerve and its branches, i.e. pain induced by nerve stretch.

Anisotropic nature of peripheral nerves and the effect on shear wave velocity. Peripheral nerve trunks are relatively complex layered structures, consisting of axons that are contained within layers of connective tissue (reviewed in [28]). As an anisotropic tissue, nerve trunks are similar to muscle and tendon, and therefore the calculation of shear-wave velocity and its relationship to the Young modulus can only be considered an estimate.[29] Particularly for anisotropic structures, shear-wave measurements will be affected by the orientation of the transducer relative to nerve fiber direction. In this study, we imaged nerves longitudinally, and therefore our measurements of shear-wave velocity are biased towards those waves that pass parallel to the nerve fibers within the nerve trunk. As such, shear-waves may be subjected to a wave-guide effect, and therefore diameter of the nerve may influence velocity. Thus, the observed increase in median nerve shear-wave velocity in the forearm compared to upper arm may be partly explained by nerve size. However, the difference in median nerve cross-sectional area at these locations is relatively small (~1mm^2).[31]

When a nerve is in a non-tensioned position, fascicles are less straight.[27, 31, 32] Under tension, fascicles assume a straight course, and it is possible that this change in nerve architecture could influence shear-wave velocities. However, the differences in median nerve shear-wave velocity between 2 stretched positions (positions 3 and 4) clearly indicate a significant increase in stiffness with additional stretch. The angle of incidence, which is important to obtain clear images, will also affect shear-wave measurements. Therefore, every effort was made to always position the ultrasound beam perpendicular to the nerve. On analysis, the small differences in overall nerve angle relative to the transducer (<12°) did not affect shear-wave velocity.

The effects of age, height and weight on shear-wave velocity. The trend towards a decreased shear-wave velocity in nerve tensioned positions in subjects over age 40 years was unexpected, since, paradoxically, the collagen content and thickness of the perineurium has been shown to increase with age.[33-35] It is possible that a decrease in shear-wave velocity is the result of a change in nerve architecture caused by disorganization or fragmentation of collagen fibrils that is known to occur with increasing age (e.g.[36]). Collagen within the nerve sheath is thought to 'cushion' the axons from compression,[32] and consequently the degradation of collagen may be partially responsible for the

reported increase of peripheral nerve compression neuropathy with age.[37] A decrease in tissue stiffness with age has been reported in elastography studies of tendons.[38]

For the median nerve, shear-wave velocities were not affected by gender, height, or weight. However, for the tibial nerve, there was a positive correlation between height and shear-wave velocity in position 2, possibly indicating an increase in nerve tension in taller individuals. Interestingly, with the nerve in the slack position (position 1) there was a significant increase in shear-wave velocities in men compared to women. Only 2 of the 26 subjects were considered obese, with a body mass index over 30. This factor is important, since adipose tissue can attenuate the ultrasound signal and the ability to provide an accurate estimation of tissue stiffness.[39] A larger study is required to confirm these findings.

Reliability and the effects of probe pressure on shear-wave velocity. Shear-wave elastography removes much of the operator dependence that is associated with static elastography. Intraclass correlation coefficients (ICC) as an indicator of reliability for measurement of nerve shear-wave velocity ranged from 0.39 to 0.69, indicating fair to substantial reliability.[40] The ICCs in this study are lower than those obtained for the tibial nerve by Andrade and colleagues. However, there were several differences between studies that may in part account for this dissimilarity, for example, the scanner used, the sequence of limb positioning, and the repeat measurement protocol employed. Consistent with our ICC values, within-subject standard deviations for nerve shear-wave velocity were low in each limb position. Furthermore, repeated testing of the same subjects on different days demonstrated excellent reliability. Since both the median and tibial nerve trunks are fairly superficial, increased probe pressure during imaging could introduce an unintended variable. Although there was no significant difference in velocity with different degrees of probe pressure, all imaging was carried out using ‘moderate’ probe pressure. As an indication of pressure, the change in nerve depth was measured. During these experiments, the depth changed by only 7.4% compared to the ‘light’ probe pressure position. Other variables that may affect tissue stiffness include exercise, although none of the subjects had exercised vigorously prior to imaging.

Clinical impact. We have shown that in postures that stretch peripheral nerves there is an increase in shear-wave velocity and therefore stiffness. As such, shear-wave elastography may be a useful tool for examining nerve biomechanics in healthy individuals and in patients with signs of a nerve movement restriction, e.g. carpal tunnel syndrome. Intrinsic changes in neural architecture, such as remodeling of collagen, intraneural edema, or thickening of the perineurium, also affect nerve stiffness.[41-44] Therefore, shear-wave elastography should be helpful for identification of these changes in conditions where clinical tests that stretch peripheral nerves are painful, such as diabetic neuropathy,[45] chronic whiplash,[3] and non-specific arm pain.[47]

In the clinical setting, the successful application of shear-wave elastography depends on being able to easily visualize the nerve. We have shown that when imaged in longitudinal orientation and in limb positions that tension the nerve trunk, a clear delineation of the nerve structure from the surrounding tissue is possible. This delineation may be extremely important for visualization of peripheral nerves during, for example, ultrasound-guided anesthesia.[48] Finally, the observed changes in nerve shear-wave velocity in different limb positions suggests that care needs to be taken with overall limb posture during imaging, as this may be a confounding factor.

Acknowledgements

We would like to acknowledge Siemens Healthcare for the loan of the Acuson S2000 ultrasound and to Professor Bruce Lynn for his helpful comments on the manuscript.

Abbreviations

ROI Region of interest

References

1. Boyd BS, Dilley A. Altered tibial nerve biomechanics in patients with diabetes mellitus. Muscle Nerve 2014;50:216-223.

2. Dilley A, Lynn B, Pang SJ. Pressure and stretch mechanosensitivity of peripheral nerve fibres following local inflammation of the nerve trunk. Pain 2005;117:462-472.

3. Greening J, Dilley A, Lynn B. In vivo study of nerve movement and mechanosensitivity of the median nerve in whiplash and non-specific arm pain patients. Pain 2005;115:248-253.

4. Majlesi J, Togay H, Unalan H, Toprak S. The sensitivity and specificity of the Slump and the Straight Leg Raising tests in patients with lumbar disc herniation. J Clin Rheumatol 2008;14:87-91.

5. Kwan MK, Wall EJ, Massie J, Garfin SR. Strain, stress and stretch of peripheral nerve. Rabbit experiments in vitro and in vivo. Acta Orthop Scand 1992;63:267-272.

6. Lundborg G. 1988. Nerve Injuries and Repair. Churchill Livingstone: Edinburgh.

7. Millesi H, Zöch G, Rath T. The gliding apparatus of peripheral nerve and its clinical significance. Ann Chir Main Memb Super. 1990;9:87-97.

8. Hough AD, Moore AP, Jones MP. Reduced longitudinal excursion of the median nerve in carpal tunnel syndrome. Arch Phys Med Rehabil 2007;88:569-576.

9. Korstanje JW, Scheltens-De Boer M, Blok JH, Amadio PC, Hovius SE, Stam HJ*, et al.* Ultrasonographic assessment of longitudinal median nerve and hand flexor tendon dynamics in carpal tunnel syndrome. Muscle Nerve 2012;45:721-729.

10. Erel E, Dilley A, Greening J, Morris V, Cohen B, Lynn B. Longitudinal sliding of the median nerve in patients with carpal tunnel syndrome. J Hand Surg [Br] 2003;28:439-443.

11. Dilley A, Odeyinde S, Greening J, Lynn B. Longitudinal sliding of the median nerve in patients with non-specific arm pain. Man Ther 2008;13:536-543.

12. Palmeri ML, Dahl JJ, MacLeod DB, Grant SA, Nightingale KR. On the feasibility of imaging peripheral nerves using acoustic radiation force impulse imaging. Ultrason Imaging 2009;31:172-182.

13. Nightingale K. Acoustic Radiation Force Impulse (ARFI) Imaging: a Review. Curr Med Imaging Rev 2011;7:328-339.

14. Chen XM, Cui LG, He P, Shen WW, Qian YJ, Wang JR. Shear wave elastographic characterization of normal and torn achilles tendons: a pilot study. J Ultrasound Med 2013;32:449-455.

15. Aubry S, Nueffer JP, Tanter M, Becce F, Vidal C, Michel F. Viscoelasticity in Achilles tendonopathy: quantitative assessment by using real-time shear-wave elastography. Radiology 2015;274:821-829.

16. Chino K, Takahashi H. The association of muscle and tendon elasticity with passive joint stiffness: In vivo measurements using ultrasound shear wave elastography. Clin Biomech 2015; 30:1230-1235.

17. Cortes DH, Suydam SM, Silbernagel KG, Buchanan TS, Elliott DM. Continuous Shear Wave Elastography: A New Method to Measure Viscoelastic Properties of Tendons in Vivo. Ultrasound Med Biol 2015;41:1518-1529.

18. Haen TX, Roux A, Labruyere C, Vergari C, Rouch P, Gagey O*, et al.* Shear wear elastography of the human Achilles tendon: a cadaveric study of factors influencing the repeatability. Comput Methods Biomech Biomed Engin 2015;1-2.

19. Nordez A, Hug F. Muscle shear elastic modulus measured using supersonic shear imaging is highly related to muscle activity level. J Appl Physiol 2010;108:1389-1394.

20. Yoshitake Y, Takai Y, Kanehisa H, Shinohara M. Muscle shear modulus measured with ultrasound shear-wave elastography across a wide range of contraction intensity. Muscle Nerve 2014;50:103-113.

21. Miyamoto H, Halpern EJ, Kastlunger M, Gabl M, Arora R, Bellmann-Weiler R*, et al.* Carpal tunnel syndrome: diagnosis by means of median nerve elasticity--improved diagnostic accuracy of US with sonoelastography. Radiology 2014;270:481-486.

22. Liao YY, Lee WN, Lee MR, Chen WS, Chiou HJ, Kuo TT*, et al.* Carpal tunnel syndrome: US strain imaging for diagnosis. Radiology 2015;275:205-214.

23. Ogur T, Yakut ZI, Teber MA, Alp F, Turan A, Tural A*, et al.* Ultrasound elastographic evaluation of the median nerve in pregnant women with carpal tunnel syndrome. Eur Rev Med Pharmacol Sci 2015;19:23-30.

24. Ishibashi F, Taniguchi M, Kojima R, Kawasaki A, Kosaka A, Uetake H. Morphological changes of the peripheral nerves evaluated by high-resolution ultrasonography are associated with the severity of diabetic neuropathy, but not corneal nerve fiber pathology in patients with type 2 diabetes. J Diabetes Investig 2015;6:334-342.

25. Kantarci F, Ustabasioglu FE, Delil S, Olgun DC, Korkmazer B, Dikici AS*, et al.* Median nerve stiffness measurement by shear wave elastography: a potential sonographic method in the diagnosis of carpal tunnel syndrome. Eur Radiol 2014;24:434-440.

26. Andrade RJ, Nordez A, Hug F, Ates F, Coppieters MW, Pezarat-Correia P*, et al.* Non-invasive assessment of sciatic nerve stiffness during human ankle motion using ultrasound shear wave elastography. J Biomech 2015; [Epub ahead of print]

27. Dilley A, Lynn B, Greening J, DeLeon N. Quantitative in vivo studies of median nerve sliding in response to wrist, elbow, shoulder and neck movements. Clin.Biomech 2003;18:899-907.

28. Greening J, Dilley A, Peripheral mechanisms of chronic upper limb pain: nerve dynamics, inflammation and neurophysiology, in C. Fernandez de las Penas, J. Cleland, and P. Huijbregts, editors. Neck and Arm Pain Syndromes. Churchill Livingstone: Philadelphia, 2011.

29. Shiina T, Nightingale KR, Palmeri ML, Hall TJ, Bamber JC, Barr RG*, et al.* WFUMB guidelines and recommendations for clinical use of ultrasound elastography: Part 1: basic principles and terminology Ultrasound Med Biol 2015;41:1126-1147.

30. Cartwright MS, Shin HW, Passmore LV, Walker FO. Ultrasonographic reference values for assessing the normal median nerve in adults. J Neuroimaging 2009;19:47-51.

31. Clarke E, Bearn JG. The spiral nerve bands of Fontana. Brain 1972;95:1-20.

32. Sunderland S, 1991. Nerve Injuries and Their Repair. Churchill Livingstone: Edinburgh.

33. Ugrenovic S, Jovanovic I, Vasovic L. Morphometric analysis of human sciatic nerve perineurial collagen type IV content. Microsc Res Tech 2011;74:1127-1133.

34. Amer MG, Mazen NF, Mohamed NM. Role of calorie restriction in alleviation of age-related morphological and biochemical changes in sciatic nerve. Tissue Cell 2014;46:497-504.

35. Esquisatto MA, de Aro AA, Feo HB, Gomes L. Changes in the connective tissue sheath of Wistar rat nerve with aging. Ann Anat 2014;196:441-448.

36. Snedeker JG, Gautieri A. The role of collagen crosslinks in ageing and diabetes - the good, the bad, and the ugly. Muscles Ligaments Tendons J 2014;4:303-308.

37. Latinovic R, Gulliford MC, Hughes RA. Incidence of common compressive neuropathies in primary care. J Neurol Neurosurg Psychiatry 2006;77:263-265.

38. Hsiao MY, Chen YC, Lin CY, Chen WS, Wang TG. Reduced Patellar Tendon Elasticity with Aging: In Vivo Assessment by Shear Wave Elastography. Ultrasound Med Biol 2015;41:2899-2905.

39. Palmeri ML, Nightingale KR. What challenges must be overcome before ultrasound elasticity imaging is ready for the clinic? Imaging Med 2011;3:433-444.

40. Landis JR, Koch GG. The measurement of observer agreement for categorical data. Biometrics 1977;33:159-174.

41. Bora FW, Jr., Richardson S, Black J. The biomechanical responses to tension in a peripheral nerve. J Hand Surg (Am) 1980;5:21-25.

42. Beel JA, Groswald DE, Luttges MW. Alterations in the mechanical properties of peripheral nerve following crush injury. J.Biomech 1984;17:185-193.

43. Powell HC, Meyers RR. Pathology of experimental nerve compression. Lab Invest 1986;55:91-100.

44. Dillman JR, Stidham RW, Higgins PD, Moons DS, Johnson LA, Rubin JM. US elastography-derived shear wave velocity helps distinguish acutely inflamed from fibrotic bowel in a Crohn disease animal model. Radiology 2013;267:757-766.

45. Boyde BS, Dilley A. Altered tibial nerve biomechanics in patients with diabetes mellitus. Muscle Nerve 2014;50:216-223.

46. Greening J, Dilley A, Lynn B. In vivo study of nerve movement and mechanosensitivity of the median nerve in whiplash and non-specific arm pain patients. Pain 2005;115:248-253.

47. Dilley A, Greening J. Non-specific arm pain. In McMahon S, Koltzenburg M, Tracey I, Turk DC, editors. Wall and Melzack's Textbook of Pain, 6th Edition. Elsevier Saunders, 2013.

48. Munirama S, Joy J, Eisma R, Corner G, Cochran S, McLeod G. Shear wave elastography: novel technology for ultrasound-guided regional anesthesia. Anesthesiology. 2013;119:698.

Tables

Table 1. Demographic data.

	n	Age, years mean (range)	Weight, kg Mean (SEM)	Height, m Mean (SEM)
Men	11	37.5 (20 – 72)	81.3 (3.7)	1.80 (0.05)
Women	15	38.8 (23 – 58)	63.6 (2.5)	1.67 (0.01)
P		0.83	<0.05	<0.001

Men and Women were compared using unpaired *t*-tests.

Table 2. Intra-class correlation coefficients (ICC) for test-retest reliability of shear-wave velocities obtained from the median and tibial nerves.

		Pos1		Pos3 (MN) / Pos2 (TN)		Pos4 (MN) / Pos3 (TN)	
		ICC	95% CI	ICC	95% CI	ICC	95% CI
Median nerve	Forearm	0.59	0.36-0.77	0.52	0.28-0.73	0.41	0.16-0.65
	Upper arm	0.57	0.33-0.76	0.69	0.49-0.83	0.53	0.29-0.74
Tibial nerve		0.37	0.10-0.64	0.53	0.29-0.74	0.54	0.29-0.75

ICCs were calculated from the individual trial data as a measure of test-retest reliability. Pos = position, CI = confidence interval, MN = median nerve, TN = tibial nerve

Table 3. Within-subject standard deviations (s_w) for shear-wave velocities obtained from the median and tibial nerves.

		Pos1		Pos3 (MN) / Pos2 (TN)		Pos4 (MN) / Pos3 (TN)	
		Mean s_w	Range	Mean s_w	Range	Mean s_w	Range
Median nerve	Forearm	0.30	0.07-0.80	0.58	0.01-2.29	0.77	0.11-2.22
	Upper arm	0.27	0.04-0.55	0.35	0.06-0.88	0.97	0.15-2.07
Tibial nerve		0.38	0.07-0.90	0.38	0.07-0.90	0.83	0.04-2.15

Units = m/sec. Pos = position, MN = median nerve, TN = tibial nerve

Table 4. Repeat testing in 4 subjects.

		Median nerve (forearm)						Tibial nerve		
Subject	Repeat day	Pos3	Pos3 repeat	% diff	Pos4	Pos4 repeat	% diff	Pos2	Pos2 repeat	% diff
1	6	5.95	6.0	1%	8.54	9.39	10%	4.62	4.96	7%
2	5	5.46	5.84	7%	9.34	9.76	5%	5.61	5.83	4%
3	1	5.27	5.28	0%	8.17	8.81	8%	4.12	4.20	2%
4	12	5.73	5.85	2%	8.84	8.83	0%	6.60	5.67	-14%
Mean				2.5%			5.6%			0.2%
SD				3.0%			4.4%			9.5%

Repeat tests were carried out in positions 3 (Pos3) and 4 (Pos4) for the median nerve and position 2 (Pos2) for the tibial nerve.

Table 5. Mean (± SEM) median and tibial nerve shear-wave velocities for men and women.

	Median nerve								Tibial nerve		
	Pos1		Pos2		Pos3		Pos4		Pos1	Pos2	Pos3
	UA	FA	UA	FA	UA	FA	UA	FA			
Men	2.17 (0.11)	2.61 (0.12)	2.55 (0.16)	2.26 (0.09)	3.10 (0.18)	6.09 (0.36)	7.07 (0.56)	8.80 (0.39)	3.47 (0.18)	5.61 (0.28)	8.10 (0.42)
Women	2.26 (0.10)	2.61 (0.11)	2.61 (0.16)	2.57 (0.18)	3.10 (0.20)	5.69 (0.17)	6.59 (0.35)	8.54 (0.16)	3.08 (0.09)	4.81 (0.28)	7.15 (0.34)
P	0.54	1.00	0.79	0.25	1.00	0.29	0.46	0.51	0.05	0.06	0.09

Data have been compared using unpaired *t*-test (*P* values are shown). Pos = position, UA = upper arm, FA = forearm.

Figure Legends

Figure 1. Examples of upper and lower limb start and end positions and typical elastograms. a-b corresponds to positons 1 (a) and 4 (b) for the upper limb, showing the ultrasound probe in the upper arm and forearm. The approximate angle of the shoulder (S), elbow (E), and wrist (W) are shown. c-d corresponds to positons 1(c) and 3 (d) for the lower limb, showing the ultrasound probe at the ankle. The approximate angle of the hip (H), knee (K), and ankle (A) are shown. The ultrasound images represent the typical elastogram obtained in the upper arm and forearm in each position. The white vertical bars indicate the median (a and b) or tibial nerve (c and d). Note the increase in shear wave velocity from the slack through to the stretched positions (i.e. with increasing nerve path length). Dark blue = 0.5 m/s, Red = 10 m/s (refer to scale bar).

Figure 2. Median nerve shear-wave velocities. (a) Mean shear-wave velocity in the upper arm and mid forearm in each limb position. (b) Normalized data, expressed as percent change from position 1. (i.e. the slack position). In a, ** $P < 0.001$ (paired t test). † $P < 0.05$ compared to position 1 (repeated measures ANOVA followed by Bonferonni *post hoc* test). ‡ $P < 0.05$ compared to position 1 (unpaired *t*-test). Note position 2 was not included in the repeated measures ANOVA. In b,* $P < 0.05$, ** $P < 0.001$ (paired *t*-test). Error bars: SEM.

Figure 3. Tibial nerve shear-wave velocities. (a) Mean shear-wave velocity immediately proximal to the tarsal tunnel in each limb position. (b) Normalized data, expressed as percent change from position 1. (i.e. the slack position). † $P < 0.05$ compared to position 1 (repeated measures ANOVA followed by Bonferonni *post hoc* test). * $P < 0.05$.

Figure 4. Effects of probe pressure on shear-wave velocity. The mean median nerve shear-wave velocity (calculated from 3 repeats) is shown for 3 subjects (squares, diamonds, and triangles on graph) with varying degrees of probe pressure. “Light” refers to the probe being held above the skin with excess gel; “Moderate” refers to the probe resting on the skin with minimal pressure; “Firm” refers to the experimenter applying substantial pressure. As a measure of probe pressure, mean percent

decrease in nerve depth from “light” (± SEM) is given (*). For each subject, the shoulder was abducted to 90°, elbow fully extended, and wrist neutral. Error bars: SEM.

Figure 5. Effect of age on median and tibial nerve shear-wave velocity. (a and b) Correlation between age and median nerve shear wave velocities in positions (a) 3 and (b) 4. (c) Correlation between age and tibial nerve shear-wave velocities in positon 2. (d) Typical median nerve elastograms in positon 4 for a young and older participant.

Figure 6. Correlation between height and tibial nerve shear-wave velocities in position 2.

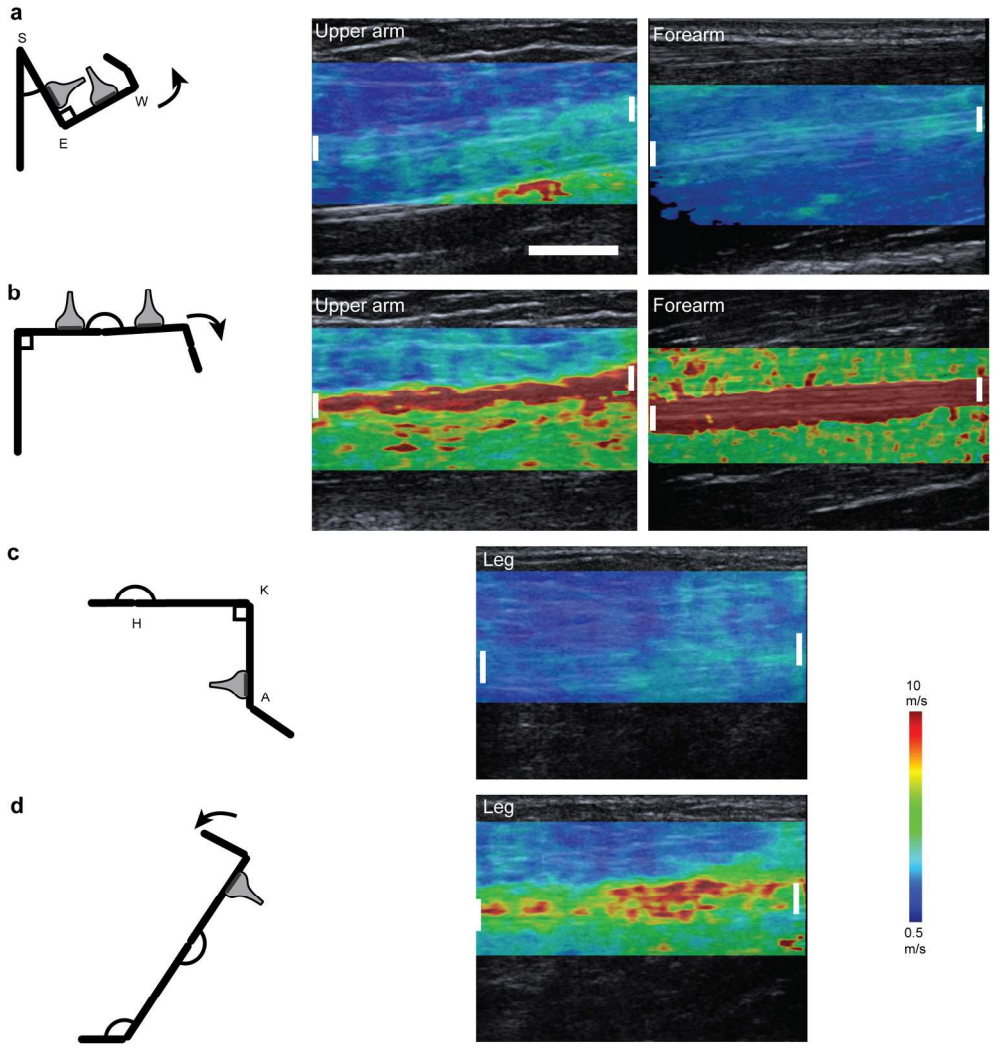

Figure 1. Examples of upper and lower limb start and end positions and typical elastograms. a-b corresponds to positons 1 (a) and 4 (b) for the upper limb, showing the ultrasound probe in the upper arm and forearm. The approximate angle of the shoulder (S), elbow (E) and wrist (W) are shown. c-d corresponds to positons 1(c) and 3 (d) for the lower limb, showing the ultrasound probe at the ankle. The approximate angle of the hip (H), knee (K) and ankle (A) are shown. The ultrasound images represent the typical elastogram obtained in the upper arm and forearm in each position. The white vertical bars indicate the median (a and b) or tibial nerve (c and d). Note the increase in shear wave velocity from the slack through to the stretched positions (i.e. with increasing nerve path length). Dark blue = 0.5 m/s, Red = 10 m/s (refer to scale bar).

185x205mm (300 x 300 DPI)

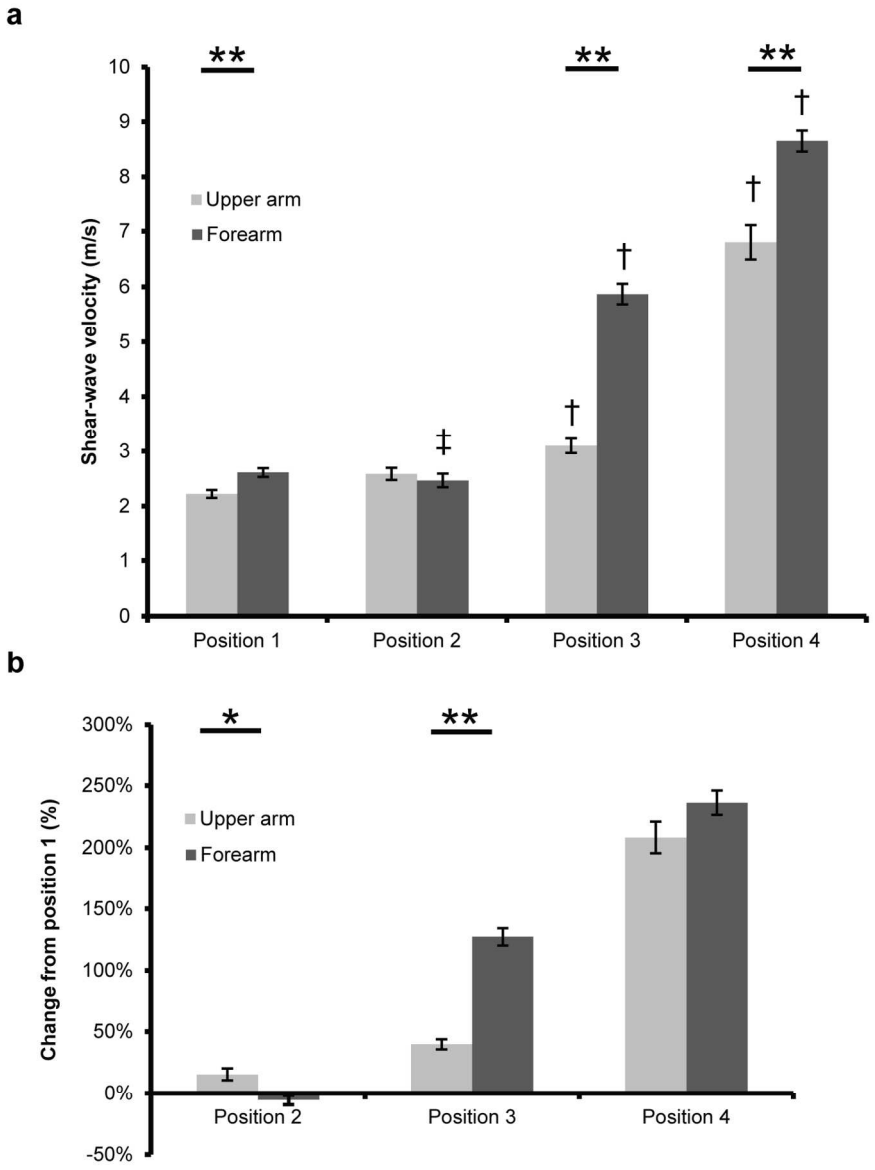

Figure 2. Median nerve shear-wave velocities. (a) Mean shear-wave velocity in the upper arm and mid forearm in each limb position. (b) Normalised data, expressed as percent change from position 1. (i.e. the slack position). In a, ** $p < 0.001$ (paired t test). † $p < 0.05$ compared to position 1 (repeated measures ANOVA followed by Bonferonni's post hoc test). ‡ $p < 0.05$ compared to position 1 (unpaired t test). Note position 2 was not included in the repeated measures ANOVA. In b,* $p < 0.05$, ** $p < 0.001$ (paired t test). Error bars = SEM.

131x167mm (300 x 300 DPI)

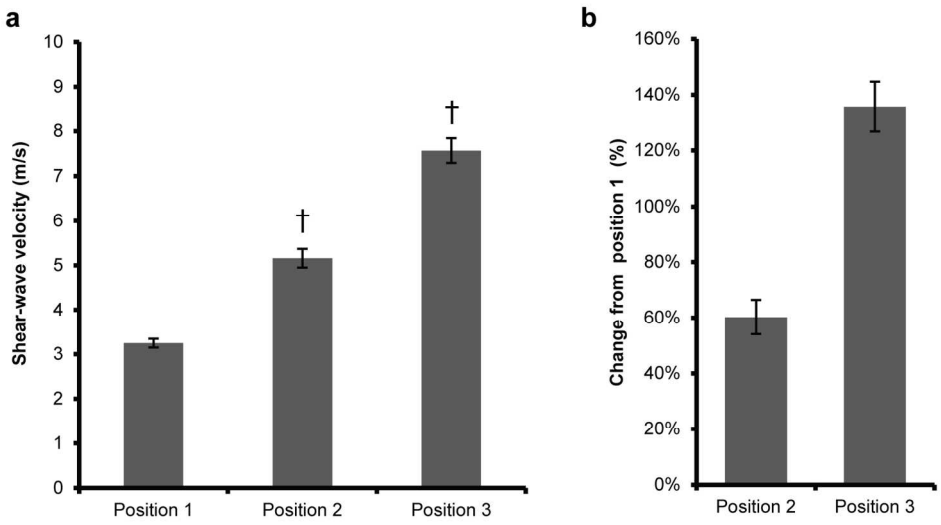

Figure 3. Tibial nerve shear-wave velocities. (a) Mean shear-wave velocity immediately proximal to the tarsal tunnel in each limb position. (b) Normalised data, expressed as percent change from position 1. (i.e. the slack position). † $p < 0.05$ compared to position 1 (repeated measures ANOVA followed by Bonferonni's post hoc test). * $p < 0.05$.

153x81mm (300 x 300 DPI)

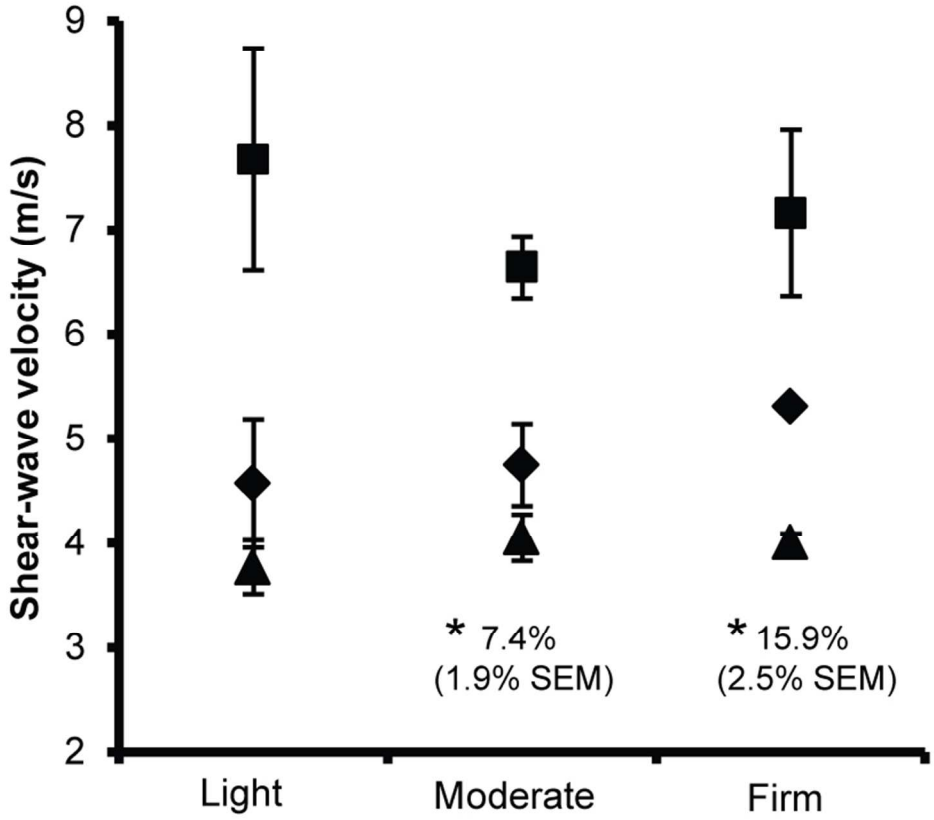

Figure 4. Effects of probe pressure on shear-wave velocity. The mean median nerve shear-wave velocity (calculated from three repeats) is shown for three subjects (square, diamond and triangle on graph) with varying degrees of probe pressure. "Light" refers to the probe being held above the skin within excess gel; "moderate" refers to the probe resting on the skin with minimal pressure; "Firm" refers to the experimenter applying substantial pressure. As a measure of probe pressure, mean percent decrease in nerve depth from "light" (+/- SEM) is given (*). For each subject, the shoulder was abducted to 90°, elbow fully extend and wrist neutral. Error bars = SEM.

73x71mm (300 x 300 DPI)

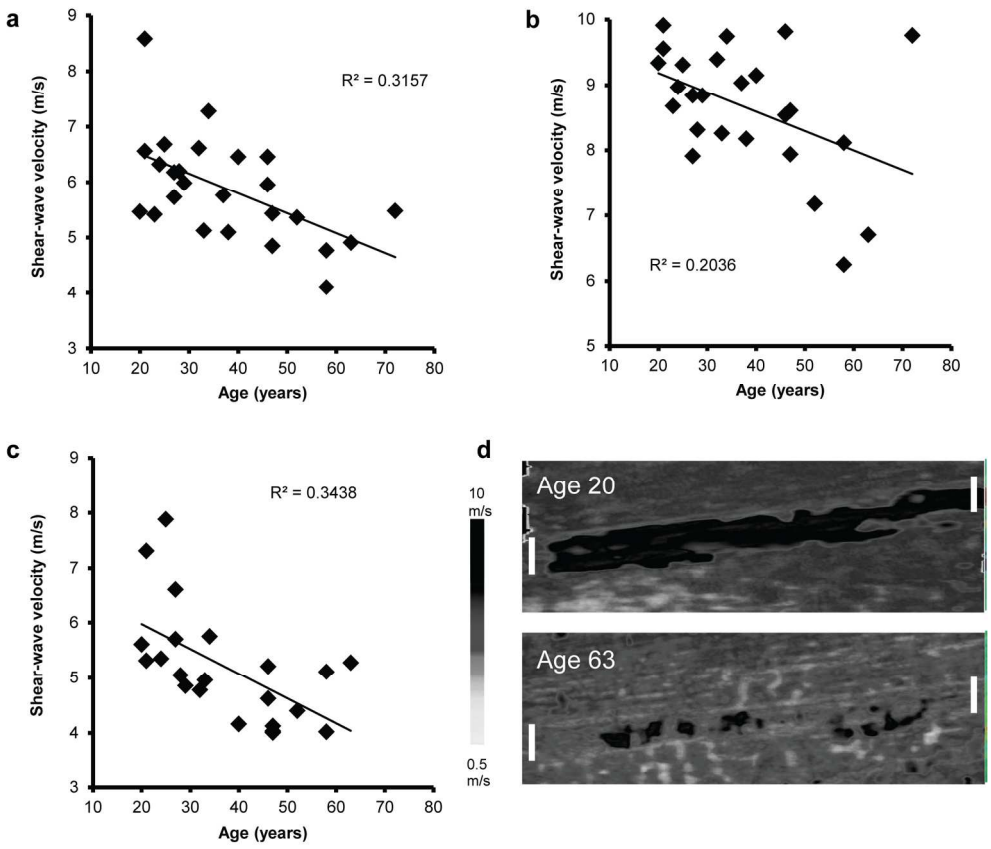

Figure 5. Effect of age on median and tibial nerve shear-wave velocity. (a and b) Correlation between age and median nerve shear wave velocities in positions (a) 3 and (b) 4. (c) Correlation between age and tibial nerve shear-wave velocities in positon 2. (d) Typical median nerve elastograms in positon 4 for a young and older participant.

170x148mm (300 x 300 DPI)

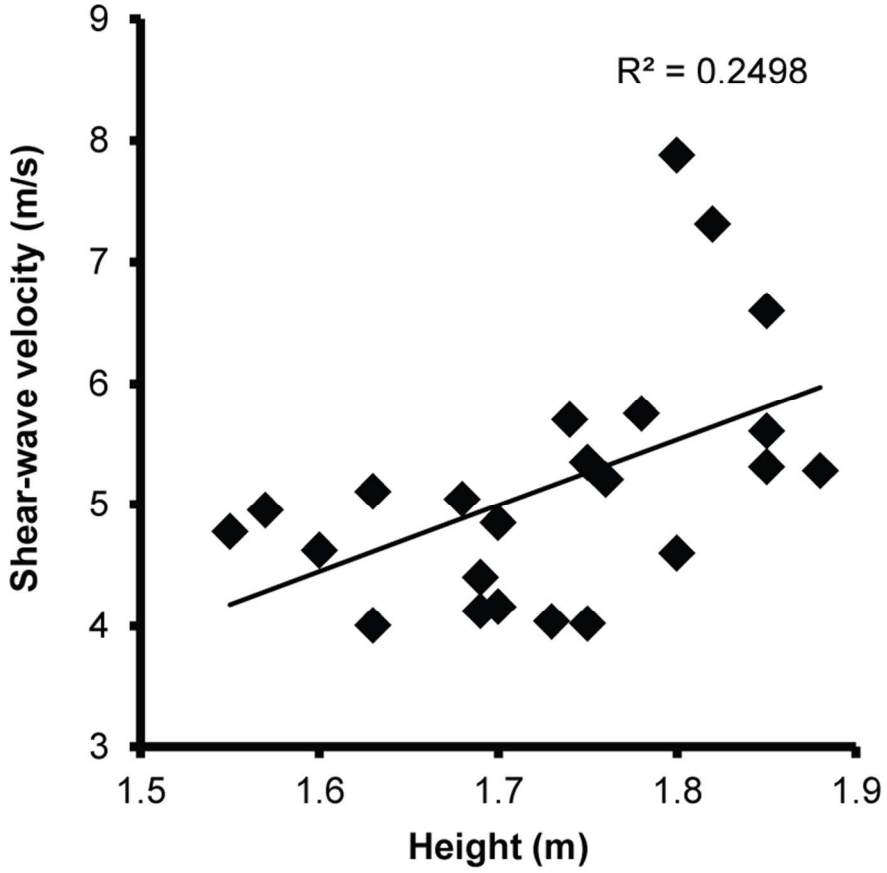

Figure 6. Correlation between height and tibial nerve shear-wave velocities in position 2.

76x73mm (300 x 300 DPI)